Optimization of Cr Seed Layer Effect for Surface Roughness of As-Deposited Silver Film using Electron Beam Deposition Method

[1]Naseem Abbas*, [2]Muzamil Hussain, [3]Nida Zahra, [4]Hassaan Ahmad, [5]Syed Muhammad Zain Mehdi,
[6]Uzair Sajjad and [6]Mohammed Amer

[1]*Department of Mechanical Engineering, University of Central Punjab, Lahore-54000-Pakistan.*
[2]*Department of Mechanical Engineering, NFC Institute of Engineering and Technology,*
Multan-60000-Pakistan.
[3]*Department of Physics, Government College University, Faisalabad-38000, Pakistan.*
[4]*Department of Technology, University of Lahore, Lahore-54000-Pakistan.*
[5]*Department of Nanotechnology and Advanced Materials Engineering, Sejong University, Seoul 05006, Korea.*
[6]*Department of Mechanical Engineering, National Chiao Tung University, Hsinchu, Taiwan.*
naseem.abbas@ucp.edu.pk*

Summary: The surface roughness is an important parameter in determining the physical properties and quality of thin films deposited by physical vapor deposition (PVD) method. The presence of an intermediate layer between metallic nanoparticles and substrate significantly promotes the adhesion and reduces the surface roughness. In this article, we have investigated the effect of Chromium (Cr) seed layer to optimize the surface roughness on the growth of as-deposited silver (Ag) film using borosilicate glass and silicon wafer substrates. For this purpose, Ag thin films were deposited with a Cr seed layer of different thickness on borosilicate glass and silicon wafer substrates using an electron beam (E-Beam) deposition method. The Cr thin film of different thickness ranging from 1 nm to 6 nm was thermally evaporated and pure Ag with the same thickness was evaporated at the same rate on previously coated substrates. The deposition of the nanostructured thin film was confirmed by UV-Vis and XRD characterizations. The difference in transmittance for uncoated and coated substrates ensured the deposition. The presence of pure Ag crystalline phase was confirmed by XRD pattern. Surface roughness was measured using Atomic Force Microscopy (AFM) and the conductance was measured using 4-probe conductivity method. The density of nanoparticles and smoothness were visualized from two dimensional (2D) and three dimensional (3D) surface height histograms of representative AFM images. The quantitative roughness was measured in terms of root mean square (RMS) roughness and mean roughness. The high dense and smoother thin films were found for ~2-4 nm Cr layer thickness in case of the glass substrate. The slight increase in roughness was observed for ~1-6 nm Cr layer thickness in case of the silicon substrate. The dependence of the conductivity of thin films on surface roughness is investigated to verify the effect of surface roughness on different applications of Ag thin film. The conductance results have been analyzed as; for a glass substrate, conductivity was maximum for thin films containing ~2 nm Cr seed layer thickness, while for silicon substrate the maximum conductivity was found for the thin film containing ~1 nm Cr seed layer.

Introduction

Surface roughness is an important parameter for determining the surface morphology, which is needed for confirming suitability of surface for its function. Surface morphology includes surface finish, surface shape, surface area roughness (Sa), or in surface profile roughness (Ra), structural characterization, asperity, and surface texture. Several preparation conditions and growth techniques would lead to a wide range of film microstructures and interface/surface morphologies that are inherently associated with different growth methods; the film deposition may not grow in a layer-by-layer manner and rough surface is produced instead of growth. Surface roughness has a direct effect on the electrical, mechanical and optical quality of thin film devices and becomes a significant parameter for solid thin films that are prepared for optical wave-guides [1, 2] multilayer interference filters [3, 4] and optical resonant filters [5, 6].

Numerous metals and metal oxides from the periodic table were used as a seed layer such as Nickel (Ni) [6], Copper (Cu) [7], Tantalum (Ta) [8], Zinc oxide (ZnO) [9], and Titanium oxide (TiO2) [10] etc for the improvement of the adhesion of the main layer to the substrate. According to our knowledge until the write-up of this paper, the best seed layer metal is the Cr metal explained by Marietta Seifert *et al.,* [11] after comparison of Titanium, Chromium, Tungsten, Platinum, and Tantalum but he did not optimize the Cr seed layer thickness. In our research, we optimize the

---

thickness of Cr seed layer for getting the optimized surface roughness of as-deposited Ag film which has not been studied yet. We select the Ag film because of its peculiar properties and widely applications in optical devices [12, 13], solar devices [14, 15], sensors [16], electronic [17], plasmonic devices [18], and antibacterial areas [19]. The performance of Ag thin film is sensitively dependent on texture, size, composition, and spacing between nanostructures [20], [21]. Although many devices were successfully developed using Ag films, the performance of such devices was deteriorated by the tendency to form isolated islands and to duet due to roughness [22, 23]. This problem was occurred due to the limited adhesive ability of metallic nanoparticles on silicon or glass substrate [21]. The nanostructured hematite films modified with Au nanoparticles were prepared to enhance the performance of photoanodes for solar water oxidation [24] and solar cells [25]. The deposition was achieved by electron beam evaporation due to the large angle between the electron beam and substrate. The photoelectrochemical performance of hematite films was optimized by controlling the preparation conditions including annealing temperature, film thickness and performing evaporation under oblique conditions. It has been also proven from many theoretical and experimental studies that the presence of an intermediate layer between metallic nanoparticles and substrate significantly promote the adhesion ability [23], [26, 27].

The influence of thin evaporated germanium (Ge) seed layer [27] on an oxide-coated or silicon substrate was investigated for depositing smooth Ag films. The presence of Ge seed layer improved the growth kinetics of deposited Ag film with surface morphology and conductivity. Instead of Ge, Chromium (Cr) interlayer [28] was introduced to increase the adhesion ability of Ag nanoparticles on a glass substrate. An effect of Cr Seed layer [26] on optical properties and microstructure of Ag thin film on the glass substrate was studied using XRD and spectrophotometer. The results showed that introducing a Cr seed layer enhanced the reflectivity and smoothness of Ag thin films. The effect of Cr seed layer [21] on optical properties of hybrid Au-Ag nanoparticles was also systematically studied using numerical method and experiment. The hybrid nanostructure with different thickness of Cr intermediate layer was fabricated. The increase in surface plasmon resonance and refractive index sensitivity was observed with increasing Cr intermediate layer thickness. These systematic studies have confirmed the improving effect of Cr interlayer on the growth of Ag thin films, motivating this comprehensive study for optimization. In addition, the basic phenomena's of nano structures

fabrication for multiple applications were also explained in the literature [29-33].

The main objective of this investigation was to compare the effect of different thickness of Cr seed layers for Ag thin films deposited on glass and silicon substrate. As the seed layer is the most important parameter for adhesion between the substrate and the required materials for many laboratory and industrial applications particularly in a chemical and biological application. So, we optimize the seed layer between the glass/ silicon wafer substrate to get the surface roughness with maximum conductivity. The UV-vis and XRD. The Ag thin films were characterized in terms of surface roughness and conductance by Atomic Force Microscopy (AFM) and four probe methods respectively. With such scale deposition, we have found the optimize seed layer thickness of Cr with improved film quality and substrate adhesion which in turn also increased the conductivity of as-grown Ag samples.

Experimental

The Cr (99.999%, Silkroute Minerals, Pakistan) seed layer and Ag (R &D research and testing / analysis) thin films were fabricated on glass (Donghai Kaiwang Quartz Product CO., LTD) and silicon wafer (p-type, 100, 1-100 Ω-cm) substrates using electron beam evaporation method by electron beam evaporator (Ningbo Leadmed Technology Co., Ltd.). Electron beam evaporation concentrates a large amount of heat produced by high energy electron beam bombardment on the source material to be deposited. The electron beam is generated by an electron gun that uses the thermoionic emission of electrons produced by an incandescent filament. A magnet focuses and bends the electron trajectory so that the beam is accelerated towards a graphite crucible (Liaoyang Hongtu Company LTD.) containing the source material. As the beam rotates and hits the surface of the source material, heating and vaporization occur. The vapor flow then condenses onto the substrate surface located at the top of the vacuum chamber. One can increase coating density by increasing the time of electron beam evaporation, possibly creating thicker coatings and thus, altering surface roughness. This whole mechanism was also pretty explained by the schematic in Fig. 1.

Prior to deposition of Cr and Ag thin films, all the glass and silicon wafer substrates were cleaned by using the acetone, isopropyl alcohol (IPA), and DI water. The source to substrate distance was fixed at 20 cm. During the deposition process, high vacuum conditions ~1.5× 10-6 Torr have been achieved, and the deposition was done at a rate of ~ 0.9 Å/s on the substrates with no rotation of the substrate. The overall

thickness of thin films was monitored throughout the deposition process by using quartz microbalance (QMB 200 monitor, crystal: 6 MHz, non-magnetic with 10mm diameter), positioned at a normal incident angle to the vapor source. To investigate the effect of Cr seed layer on the as-deposited Ag film, the surface roughness and the conductivity were measured. For this study, six borosilicate glass substrates and six silicon wafer substrates samples were used to check the seed layer effect on both substrates for comparison. For this purpose. First Cr seed layer with a thickness of ~1-6 nm was deposited on the glass and silicon substrates and then Ag thin film with same deposition rate. E-Beam deposited Ag thin film with 20 nm thickness was monitored in all samples. The schematic diagram representing the detail of samples is shown in Fig. 2.
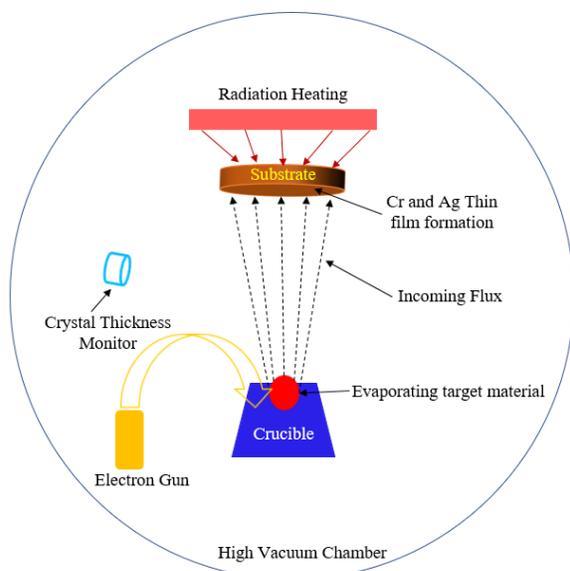
Fig. 1:   Schematic diagram of the electron beam evaporation process used in this study to create nanometer surface features on glass and silicon wafer substrate
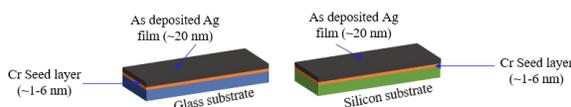
Fig. 2:   Schematic diagram of the electron beam evaporation process used in this study to create nanometer surface features on glass and silicon wafer substrate

To confirm the elemental deposition of Cr-Ag thin film the X-ray diffraction (XRD) patterns were recorded on Empyrean diffractometer using a Cu tube operated 40 kV and 30 mA. The diffraction data were recorded in the range of Bragg angles

10.02-70.98º. All XRD measurements were taken on ambient temperatures. The optical transmission spectra of the coated and uncoated substrate were acquired using Cary 5000 UV-Vis-NIR spectrophotometer.

To investigate the surface morphology, all the samples were characterized by an Atomic force microscope (AFM) with a scan size of 5 μm × 5 μm scan size at ambient conditions. The collected image's data were analyzed qualitatively and quantitatively using the Gwyddion software. The 2D and 3D images data were characterized and surface roughness in term of root mean square roughness (Sq) and mean roughness (Sa) was measured quantitatively for getting a better comparison of Cr seed layer thickness on glass and silicon substrate.

The electrical conductivity of the thin film was measured using a four-point probe apparatus at room temperature. A constant current (I) from the current source was passed through the outer pair of probe tips and potential drop (V) was measured across two inner probe tips. The current and voltage were measured using a digital panel meter and power supply unit. The resistivity (ρ) was measured using equation 1.

$$\rho = \frac{V}{I} tCF$$
(1)

where t is the thickness of the sample and CF is geometrical correction factor. CF=π/ln2, when the spacing between probe tips is very small than the dimension of the sample. The electrical conductivity (σ) was measured by equation 2.

$$\sigma = \frac{1}{\rho}$$
(2)

Results and Discussion

XRD and UV-Vis Characterizations

The transmittance spectrum obtained from uncoated and Ag-coated Si substrate with the variation of Cr seed layer thickness is shown in Fig. 3. The transmittance spectrum on the bare substrate is 100% on 200 nm wavelength while for Ag and Ag-Cr thin film deposition the significant reduction in transmittance was observed probably due to the reflection behavior of Ag deposited films. The higher transmittance was observed on the majority of wavelength. The transmittance spectrum obtained from uncoated and Ag-coated glass substrate with the

variation of Cr seed layer thickness is shown in Fig. 4. The transmittance for glass substrate is approximately 100% while it decreased from 100 to zero within the range of approximately 100 nm wavelength variation. A little variation was observed with the variation of a small range of Cr layer thickness. The deference in UV-Vis spectra for uncoated and coated substrates confirmed the deposition of nanostructured films. Moreover, the deposition was confirmed by XRD. The XRD pattern for the silicon substrate is shown in Fig.5. The basic characteristic of investigated thin films is the presence of a pure Ag crystalline phase found in all samples. The increase in peak was observed with Cr seed layer thickness.
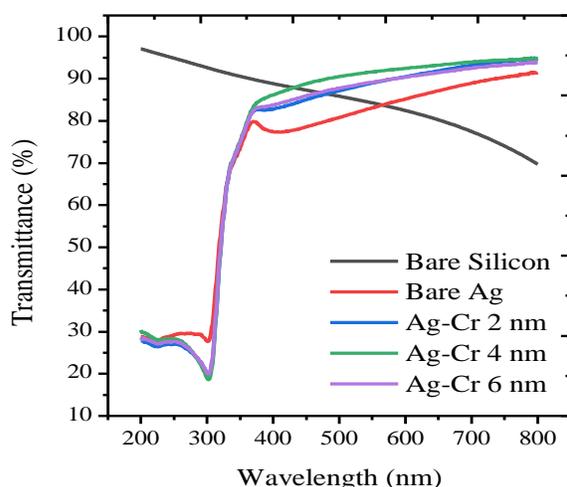
Fig. 3:   Variation of Transmittance with wavelength for Cr – seed layer on a silicon substrate.
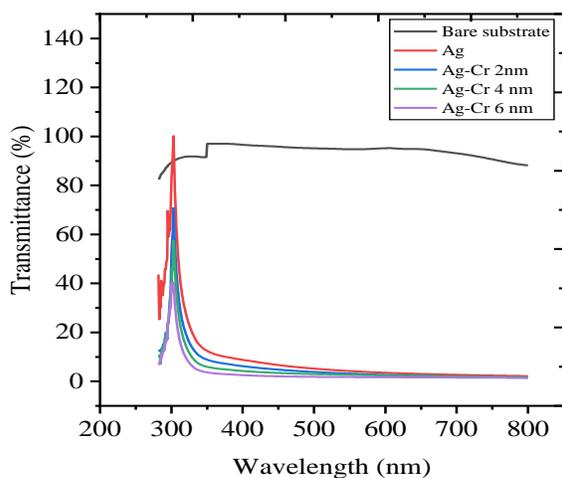
Fig. 4:   Variation of Transmittance with wavelength for Cr – seed layer on a glass substrate.
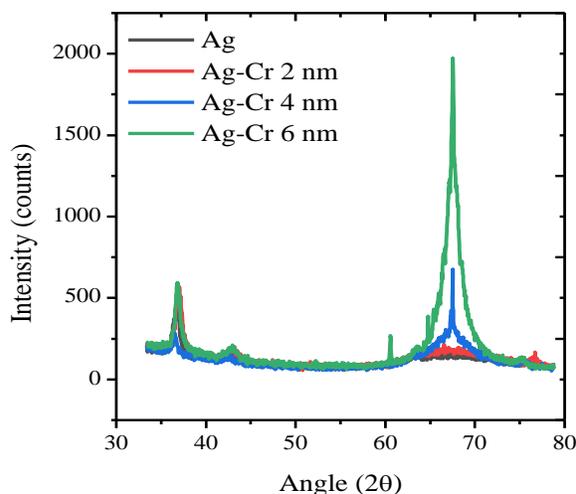
Fig. 5:   Variation of intensity with an angle for Cr – seed layer on a glass substrate using XRD.

Surface Roughness features by atomic force microscopy (AFM)

Surface roughness is a measure of surface irregularity or unevenness along out of the plane of a thin film. They play a key role in transport & optical properties like by inducing surface states, traps, scattering sites, etc. to name a few. The roughness for thin films is widely reported in two ways, one is average roughness and other is the root mean square (rms) roughness. They represent the deviation of hillocks and valleys (or pits) on the film surface from a reference plane. Avg. roughness is simply the avg of positive (hillocks deviation) and negative (valley deviation) values from the reference plane. Which is not truly reflecting the surface deviation? We also calculate the rms and means roughness of each sample discussing in this article and compared all the samples with a different thickness of Cr on the glass and silicon substrates and got the optimized Cr seed layer thickness on as-deposited silver film.

The representative AFM data of Ag thin films on glass and silicon substrates is shown in Fig. 6 and Fig.7 respectively. The two-dimensional (2D) surface height data is represented in the first column of these figs, while the second column is representing the three-dimensional (3D) peak height histograms of representative AFM image. For all samples surface roughness measurements, we used portable AFM (The physlab, Lahore University of Management Sciences-Pakistan), having very high resolution ~ 0.16 nanometer with different operational modes. The density of nanoparticles and smoothness can be visualized from the representative images. The quantitative measured values of root mean square

(RMS) roughness and mean roughness are given in Table-1. For glass substrate, the RMS roughness and mean roughness were found the minimum for Cr thickness of 2 nm. The values of roughness for 3 nm and 4 nm were also found in a small range near to the thickness of 2 nm. The increase in roughness was observed when Cr layer thickness increases from 4nm. Its surface topography was clearly shown in Fig. 6.

of 1 nm and the little increase in roughness was observed for samples having a thickness of 2 nm to 6 nm. However, the difference in values of roughness was found smaller as compared to the glass substrate. It means homogeneity was higher as compared to the glass substrate. The variation of mean roughness with a variation of Cr seed layer thickness on a silicon substrate was shown in Fig. 7.

Fig. 6: Surface topography of as-deposited Ag thin film with Cr seed layer effect on glass substrates.
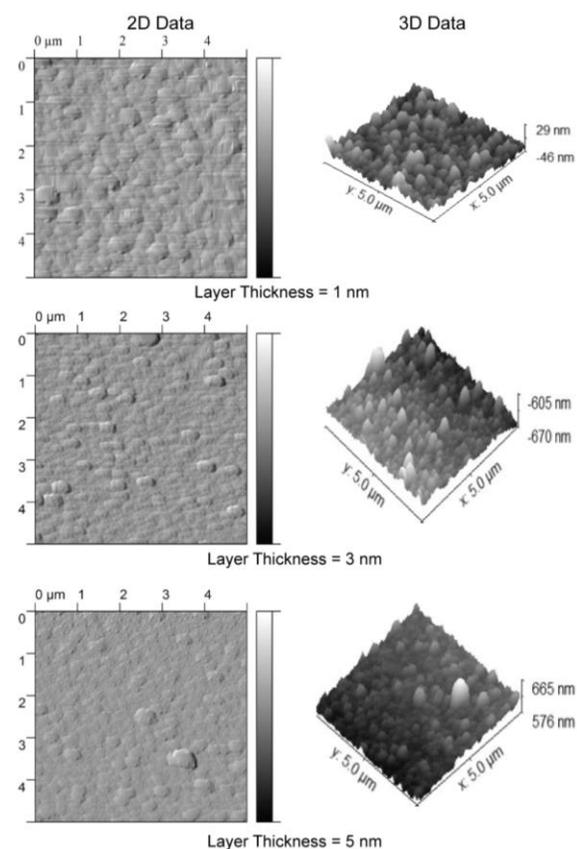
Fig.7: Surface topography of as-deposited Ag thin film with Cr seed layer effect on silicon substrates.

Table-1: The quantitative values of roughness using AFM.

Sample #	Glass substrates		Silicon Substrates	
	RMS roughness (S_q)	Mean roughness (S_a)	RMS roughness (S_q)	Mean Roughness (S_a)
1	13.30 nm	6.81 nm	8.967 nm	6.928 nm
2	3.565 nm	2.776 nm	9.173nm	7.309nm
3	3.739 nm	2.822 nm	13.24 nm	7.74 nm
4	4.336 nm	3.079 nm	13.52 nm	8.09 nm
5	14.30 nm	7.59 nm	10.53nm	8.17 nm
6	15.23nm	9.87 nm	10.57 nm	8.48 nm

For silicon substrate, the minimum roughness was observed for Cr seed layer thickness

In addition, the surface morphologies of as-deposited Ag films using a Cr seed layer were analyzed for comparison as shown in Fig.8. This graphical trend shows a novel and promising an optimized result that the surface morphologies using silicon wafer is better as compared to the glass substrate (Verified from AFM images of Fig. 6 and Fig. 7). This goodness of silicon substrate was because silicon substrate shows better local surface roughness and overall bulk flatness, homogeneity of refractive index (or differences with the film) and absence of secondary back reflection (not being transparent and thick) would make silicon a better substrate for seed layer activeness.
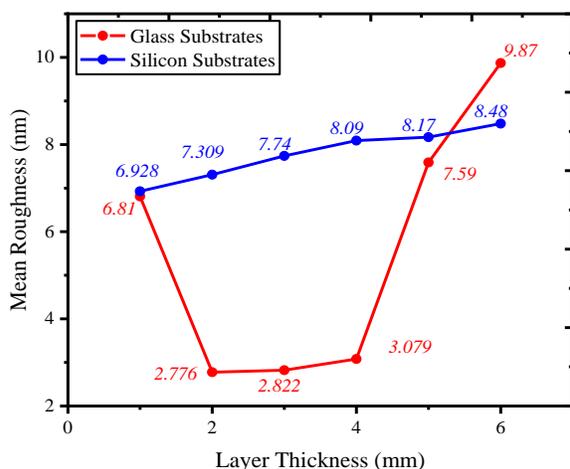
Fig. 8:   Variation of mean surface roughness with a variation of Cr seed layer thickness on the glass and silicon substrates

Conductivity analysis using four probe method

The four-point probe was applied in this experimental research as it is preferable over a two-point probe because the contact and spreading resistances associated with the two-point probe are large and the true resistivity can't be separated from the measured resistivity. In a four-point probe, a very little contact and spreading resistance is associated with the voltage probes and hence one can obtain a fairly accurate calculation of the resistivity. The use of four probe eliminates errors due to the probe resistance, the spreading resistance under each probe, and the contact resistance between each metal probe and semiconductor material. So, it was examined that the conductivity of thin films is dependent on surface roughness, as an increase in conductivity was observed with improvement in surface morphology. For a glass substrate, the conductivity of samples with 2 nm, 3 nm, and 4t nm was found higher as compared to remaining samples. For a silicon substrate, the decrease in conductivity was observed with an increase in Cr. Intermediate thickness from 1 nm to 6 nm. The values of conductivity for both substrates were given in Table-2 and Table-3. The variation of conductance with a variation of Cr seed layer thickness was shown in Fig. 9.

Table-2: Conductivity at an average value of current voltage for a glass substrate.

Cr Seed Layer	Glass substrate				
	V (V)	I (A)	t (cm)	ρ (Ωcm)	σ
1	0.550638	9.18E-10	0.1800021	4.89E+08	2.04E-09
2	0.464756	2.17E-07	0.1800022	1745715	5.73E-07
3	0.394585	1.24E-08	0.1800023	25872529	3.87E-08
4	0.543844	7.62E-09	0.1800024	58263388	1.72E-08
5	0.543039	3.87E-09	0.1800025	1.14E+08	8.74E-09
6	0.550017	6.99E-10	0.1800026	6.42E+08	1.56E-09

Table-3: Conductivity at average value of current voltage for silicon substrate.

Cr Seed Layer	Silicon Substrate				
	V (V)	I (A)	t (cm)	ρ (Ωcm)	σ
1	0.550496	6.32E-05	0.040002	1578.191	0.000634
2	0.550536	4.64E-05	0.040002	2151.426	0.000465
3	0.550055	3.78E-05	0.040002	2635.432	0.000379
4	0.969591	4.96E-05	0.040002	3540.973	0.000282
5	0.550231	2.25E-05	0.040003	4429.094	0.000226
6	0.678534	2.23E+00	0.040003	5517.566	0.000181
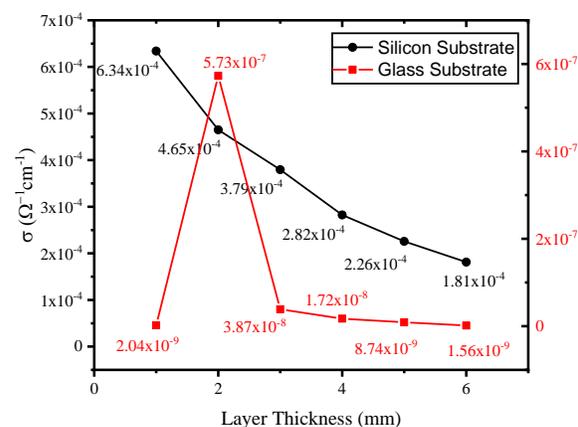
Fig. 9:   Variation of conductance with a variation of Cr seed layer thickness on the glass and silicon substrates using 4 probe conductivity method

Conclusion

The Ag thin films were characterized in terms of surface roughness and conductance. The 2D and 3D AFM data were analyzed. It was found that the introduction of 2 to 4 nm Cr layer on glass substrates promotes the growth of uniform and dense films. The surface roughness increases when the thickness of the seed layer increases from 4 nm. For silicon substrate the surface roughness little increases with the increases of Cr seed layer from 1 to 6 nm. However, variation in roughness is small for the case of the silicon substrate. The conductivity increases with the decrease of roughness. For glass substrate, the conductivity is maximum for sample 2 containing 2 nm seed layer, while for silicon substrate the maximum conductivity is achieved for 1 nm Cr seed layer. Hence for glass substrate 2 nm Cr. layer thicknesses is optimum, while for silicon substrate the optimum thickness is 1 nm. The conductance is highly dependent on surface morphology as both high conductance and smoothness are achieved at the same thickness.

Acknowledgments

of Central Punjab Lahore, Pakistan and Department of Mechanical Engineering, NFC Institute of Engineering and Technology, Multan, Pakistan by facilitating the research environment.

References

1. D. Chen, T. E. Murphy, S. Chakrabarti, and J. D. Phillips, Optical waveguiding in BaTiO3∕MgO∕AlxOy∕GaAs heterostructures, *Appl. Phys. Lett.*, **85**, 5206 (2004).
2. C. S. Evans, R. Hunneman, and J. S. Seeley, High-performance multilayer interference filters for the region 12-50μm, *J. Phys. D. Appl. Phys.*, **9**, 309 (1976).
3. J. M. Mir and J. A. Agostinelli, Optical thin films for waveguide applications, *J. Vac. Sci. Technol. A Vacuum, Surfaces, Film.*, **12**, 1439 (1994).
4. G. Castagno, F. Demichelis, and E. Minetti-Mezzetti, Design method for multilayer interference filters, *Appl. Opt.*, **19**, 386 (1980).
5. M. Niraula, J. W. Yoon, and R. Magnusson, Single-periodic-film optical bandpass filter, (2015).
6. J. Oh, H. Ryu, W.-J. Lee, and J.-S. Bae, Improved photostability of a CuO photoelectrode with Ni-doped seed layer, *Ceram. Int.*, **44**, 89 (2018).
7. S. C. Chen, S. U. Jen, R. Z. Chen, C. F. Lu, C. M. Wang, and P. C. Kuo, Effect of Cu, Cu/Ru, or Ru/Cu seed-layer on perpendicular magnetic anisotropy of Co80Pt20 films, *J. Magn. Magn. Mater.*, **459**, 106, (2018).
8. R. Law, R. Sbiaa, T. Liew, and T. C. Chong, Effects of Ta seed layer and annealing on magnetoresistance in CoFe∕Pd-based pseudo-spin-valves with perpendicular anisotropy, *Appl. Phys. Lett.*, **91**, 242504 (2007).
9. T. Tahmasebi, S. N. Piramanayagam, R. Sbiaa, R. Law, and T. C. Chong, Effect of Different Seed Layers on Magnetic and Transport Properties of Perpendicular Anisotropic Spin Valves, *IEEE Trans. Magn.*, **46**, 1933 (2010).
10. N. A. M. Asib *et al.*, Effect of TiO2 seed layer on structural and optical properties of ZnO nanostructures, in *2015 IEEE Student Conference on Research and Development (SCOReD)*, 455 (2015).
11. M. Seifert, E. Brachmann, G. K. Rane, S. B. Menzel, and T. Gemming, Capability Study of Ti, Cr, W, Ta and Pt as Seed Layers for Electrodeposited Platinum Films on γ-Al₂O₃ for High Temperature and Harsh Environment Applications., *Mater. (Basel, Switzerland)*, **10** (2017).
12. A. Rizzo, M. A. Tagliente, M. Alvisi, and S. Scaglione, Structural and optical properties of silver thin films deposited by RF magnetron sputtering, *Thin Solid Films*, **396**, 29 (2001).
13. E. Thouti, N. Chander, V. Dutta, and V. K. Komarala, Optical properties of Ag nanoparticle layers deposited on silicon substrates, *J. Opt.*, **15**, 035005 (2013).
14. A. Antonaia *et al.*, Adhesion and structural stability enhancement for Ag layers deposited on steel in selective solar coatings technology, *Surf. Coatings Technol.*, **255**, 96 (2014).
15. L. Frey, P. Parrein, L. Virot, C. Pellé, and J. Raby, Thin film characterization for modeling and optimization of silver-dielectric color filters, *Appl. Opt.*, **53**, 1663 (2014).
16. H. Tan, L. Sivec, B. Yan, R. Santbergen, M. Zeman, and A. H. M. Smets, Improved light trapping in microcrystalline silicon solar cells by plasmonic back reflector with broad angular scattering and low parasitic absorption, *Appl. Phys. Lett.*, **102**, 153902 (2013).
17. S. Baba, A. Kinbara, and M. Adachi, Island structure of sputter-deposited Ag thin films, *Vacuum*, **42**, 279 (1991).
18. R. Todorov, V. Lozanova, P. Knotek, E. Černošková, and M. Vlček, Microstructure and ellipsometric modelling of the optical properties of very thin silver films for application in plasmonics, *Thin Solid Films*, **628**, 22 (2017).
19. C.-N. Lok *et al.*, Proteomic Analysis of the Mode of Antibacterial Action of Silver Nanoparticles, *J. Proteome Res.*, **5**, 916 (2006).
20. Y. Song, J. Chen, J. Wu, and T. Zhang, Applications of Silver Nanowires on Transparent Conducting Film and Electrode of Electrochemical Capacitor, **2014**, 1–7 (2014).
21. J. Liu, H. Cai, L. Kong, and X. Zhu, Effect of Chromium Interlayer Thickness on Optical Properties of Au-Ag Nanoparticle Array, **2014**, 12 (2014).
22. E. Kudo *et al.*, Optical properties of highly stable silver thin films using different surface metal layers, *Thin Solid Films*, 0 (2018).
23. H. R. Colenso *et al.*, Comparison of seed layers for smooth, low loss silver films used in ultraviolet-visible plasmonic imaging devices, *Thin Solid Films*, **656**, 68 (2018).
24. B. Eftekharinia, A. Moshaii, A. Dabirian, and N. S. Vayghan, Optimization of charge transport in a Co-Pi modified hematite thin film produced by scalable electron beam evaporation for photoelectrochemical water oxidation, *J. Mater. Chem. A*, **5**, 3412 (2017).
25. B. Eftekharinia, A. Moshaii, N. Sobhkhiz Vayghan, and A. Dabirian, Efficient Nanoporous

Hematite Photoanodes Prepared by Electron Beam Evaporation and Au Modification, *ChemCatChem*, **10**, 4665, (2018).

26. S. Xilian and S. Jianda, Influence of Cr interlayer on the structure and optical properties of Ag films on glass substrate by magnetron sputtering, **253**, 2093 (2006).

27. L. Vj *et al.*, Ultrasmooth Silver Thin Films Deposited with a Germanium Nucleation Layer, *Nano Lett.*, **9**, 178 (2009).

28. A. J. Haes, W. P. Hall, L. Chang, W. L. Klein, and R. P. Van Duyne, A Localized Surface Plasmon Resonance Biosensor: First Steps toward an Assay for Alzheimer's Disease, *Nano Lett.*, **4**, 1029 (2004).

29. A. Benyounes, N. Abbas, M. Hammi, Y. Ziat, A. Slassi, and N. Zahra, Fabrication and characterization of novel transparent conducting oxide N-CNT doped ZnO for photovoltaic applications, *Appl. Phys. A,* **124**, 90, (2018).

30. N. Ali, and N. Abbas, Experimental investigation on the contribution of pristine multi-walled carbon nanotubes (MWCNTs) addition to the strength enhancement of cement composites, In 2017 IEEE *3rd International Conference on Engineering Technologies and Social Sciences (ICETSS)*, pp. 1-3. IEEE, (2017).

31. Z. Nida, A. Abbas, B. Saeed, N. Abbas, and M. Hussain, Synthesis and Characterization of Nd-Substituted Lithium Nickel Nano Ferrites Using Co-Precipitation Method, *Nanosci. Nnotech. Let*, **10**, 1142 (2018).

32. A. S. Jalil, Q. S. Ahmed, M. Akram, N. Abbas, A. Khalid, A. Khalil, M. L. Khalid, M. M. Mehar, K. Riaz, and M. Q. Mehmood, Fabrication of high refractive index TiO2 films using electron beam evaporator for all dielectric metasurfaces, *Mater. Res. Express,* **5**, 016410, (2018).

33. N. Ali, N. Abbas, N. Zahra, A. Hussain, and S. Q. Shabbir, Effect of multi-walled carbon nanotubes (MWCNTs) on the strength development of cementitious materials, *J. Mater. Res. Technol.* (2018).